Biochimica et Biophysica Acta 893 (1987) 349–364
Elsevier

BBA 42605

The state of detergent solubilised light-harvesting chlorophyll-*a*/*b* protein complex as monitored by picosecond time-resolved fluorescence and circular dichroism

Jonathan P. Ide [a], David R. Klug [a], Werner Kühlbrandt [b], Linda B. Giorgi [a] and George Porter [a]

[a] *Davy Faraday Research Laboratory, Royal Institution of Great Britain, and* [b] *Department of Pure and Applied Biology, Imperial College, London (U.K.)*

(Received 12 December 1986)
(Revised manuscript received 8 April 1987)

Key words: Fluorescence, picosecond; Circular dichroism; Light-harvesting complex; Energy transfer; Detergent solubilisation; C_3 symmetry

Steady-state and picosecond time-resolved fluorescence techniques in conjunction with circular dichroism have been used to study the light-harvesting chlorophyll-*a*/*b* protein complex (LHC) isolated from pea chloroplasts. In particular, the effect of changing the detergent/chlorophyll ratio on the state of the LHC has been investigated. Our results have been interpreted in light of the known protein geometry of the LHC in 2-dimensional crystals (Kühlbrandt, W. (1984) Nature 307, 478–479). The fluorescence lifetime data reveals 1/e-lifetimes of 3.53 (±0.04) ns and 1.10 (±0.01) ns for a stable, efficiently energy-transferring state of the LHC. Subnanosecond lifetimes are observed under conditions leading to aggregation, while a long component of 5.50 (±0.16) ns corresponding to free Chl *a* is found when the detergent/chlorophyll ratio is high. The circular dichroism shows a major Chl-*b* exciton, a Chl-*a*/*b* exciton and a further 'quenching' Chl-*b* exciton. These have been attributed to: a C_3 symmetric Chl-*b* interaction for which the intact C_3 protein trimer geometry is a prerequisite; a dimeric Chl-*a*/*b* interaction, the presence of which is critically dependent on the detergent type; and a further Chl-*b* interaction which arises from the presence of aggregated trimers, respectively. We have found that the degree of heterogeneity with respect to the oligomeric state of the pigment-protein trimers is dependent upon the detergent/chlorophyll ratio used. Low detergent/chlorophyll ratios result in extensive aggregation of the trimers with a geometry similar to that found in 2-dimensional crystals of the LHC. Moderate detergent conditions yield predominantly non-aggregated trimers. Excess detergent conditions result in considerable chromophore heterogeneity and loss of the main Chl-*b* exciton consistent with protein denaturation through an initial break up of the trimer geometry. From these results we believe that in vitro the minimum stable functional unit corresponds to a C_3 symmetric protein trimer.

Abbreviations: LHC, light-harvesting chlorophyll-*a*/*b* protein complex; PS I, II, Photosystem I, II; Chl, chlorophyll.

Correspondence: D.R. Klug, Davy Faraday Research Laboratory, Royal Institution of Great Britain, 21 Albemarle Street, London, W1X 4BS, U.K.

Introduction

The chlorophyll of higher plants is associated with three major macromolecular protein complexes. These are the PS I chlorophyll-protein

complex containing P-700 and approx. 120 antenna Chl-*a* molecules, a PS II complex containing P-680 and about 60 antenna Chl-*a* molecules and the light-harvesting Chl-*a*/*b* protein complex (LHC) which is responsible for 40–60% of the total thylakoid membrane chlorophyll [1].

The LHC is mainly associated with PS II and is thought to have three main functional roles. Primarily, its role is to harvest and transfer solar energy to the reaction centres of PS II. This energy migration is thought to occur by a Förster-like process [2] in which the energy is transferred through a non-radiative mechanism in a hopping motion. Each transfer step is thought to occur in a few picoseconds or less. The LHC also plays a role in controlling the distribution of absorbed quanta between the two photosystems under fluctuating external light quality [3]. It has been proposed that a sub-population of the LHC is able to move laterally from PS II-enriched appressed membranes (grana) to the stromal lamellae following phosphorylation of the LHC apoprotein [4,5]. It is also thought that this complex is involved in mediating interactions between thylakoid membranes [6]. This interaction results in the formation of thylakoid stacks and is triggered by the presence of cations.

It has been possible to form two-dimensional crystals of the LHC and, using a combination of electron microscopy and image analysis, to determine the three-dimensional structure of the LHC in the negative stain (uranyl acetate) to 16 Å resolution [7]. The 2-dimensional arrays belong to the p321 plane group, thus each unit cell comprises two LHC macromolecules with a two-fold axis of symmetry (C_2) running laterally between them. A threefold axis of symmetry (C_3) runs centrally through each macromolecular complex. The trimeric complex comprises three monomeric sub-units. The LHC monomer consists of a polypeptide which binds a number of Chl-*a* and Chl-*b* molecules, the total of which has been variously reported as 6 [8], 11 [9] and greater than 10 [10]. The ratio of Chl-*a* to Chl-*b* molecules in the complex varies between 1.1 and 1.25, suggesting the presence of 4–6 Chl-*a* and 3–5 Chl-*b* per monomer. The LHC polypeptide is the product of a small gene family [11,12] and hence is heterogeneous with respect to molecular weight. In pea, the predominant polypeptide component has a molecular weight of 25 kDa [10,11].

The principal aim of this work has been to characterise the LHC in detergent solution with regard to answering the following questions. (a) Pigment protein complex stability and efficient energy-transfer are two essential criteria characterising the LHC in vivo; under what conditions in vitro are these criteria also met? (b) For a given detergent/chlorophyll ratio what species are present in solution? Does the aggregation state of the protein vary when this ratio is changed? If so, for a given ratio, do we have predominantly one protein oligomer or is there heterogeneity with respect to the aggregation state of the protein? The characterisation of the states of the LHC in vitro under different solubilisation conditions is a critically important step before an understanding of the pigment organisation in the complex can be achieved. (c) Can we combine our knowledge of the protein geometry of the 2-dimensional LHC crystals with the spectroscopic information to suggest what the oligomeric states of the protein might be for a given detergent/chlorophyll ratio. If this can be achieved for the in vitro complex satisfying the minimum functional criteria mentioned in (a) above then it is likely that the protein geometry corresponding to the predominant species under these conditions is also that of the in vivo LHC pigment protein complex.

By changing the detergent/chlorophyll ratio we have observed a marked change in the spectroscopic properties of the protein ligated Chl-*a*/*b* molecules. We relate these observations to changes in the oligomeric state of the protein and, under extreme conditions, to the denaturation of the protein with the concomitant detachment of the associated chlorophyll molecules. Our results are discussed in relation to those obtained by Il'ina and co-workers [13], and in terms of the Van Metter-Knox-Shepanski model of the LHC [14,15]. The results obtained by Lotshaw et al. [16] will also be discussed in light of the present work.

Materials and Methods

The LHC samples were isolated from pea chloroplasts by solubilisation of thylakoids using triton X-100 as a detergent, and subsequent sucrose

density gradient centrifugation in the presence of triton X-100 [17]. The gradient fraction containing the LHC was collected and made 300 mM in KCl. The resulting microcrystalline precipitate of LHC was pelleted and washed in two changes of 100 mM KCl and one change of distilled water. Stock solutions of LHC were prepared by dissolving the dark green pellets in 1.5% (wt/vol) *n*-octyl-β-D-glucopyranoside or 0.5% triton X-100 at a Chl concentration of 1–2 mg/ml and stored in liquid nitrogen. Working solutions at detergent/chlorophyll ratios specified in Table I were prepared from the concentrated stock.

The choice of the detergent/chlorophyll molar ratios in Table I was based on results obtained from steady-state fluorescence spectra which provided information about the degree and stability of the Chl-*b* to Chl-*a* energy-transfer efficiency (see Results). The chlorophyll concentration was 10 μg/ml for all samples, corresponding to approx. $6 \cdot 10^{15}$ chlorophyll molecules per ml.

Steady-state techniques. Steady-state absorption spectra were obtained using a Perkin-Elmer 554 spectrophotometer. Steady-state fluorescence emission spectra were recorded on a Perkin-Elmer MPF4 spectrophotometer. For each of the conditions shown in Table I a steady-state fluorescence spectrum was recorded immediately after the sample was prepared from stock and again at times ranging from minutes to days after the initial preparation. The excitation wavelengths used were 470 nm (approximate Chl-*b* Soret absorption maximum, Chl *a* has a relatively small extinction coefficient at this wavelength) and 600 nm where Chl *a* and Chl *b* have nearly the same extinction coefficients. The emission was scanned from 600 nm to 740 nm.

Circular dichroism spectra were recorded on a Jasco J40CS spectropolarimeter.

Column chromatography. Free pigment in a given sample of LHC in detergent solution was estimated by column chromatography using a TSK fractogel DEAE-650 anion-exchange column equilibrated at room temperature with 10 mM phosphate buffer at pH 6.0. Under these conditions, the chlorophyll-protein complex remained bound to the column while free pigment passed through with the void volume. After washing with 0.83% *n*-octyl-β-D-glucopyranoside the chlorophyll protein complex was eluted with 140 mM sodium chloride in 0.83% *n*-octyl-β-D-glucopyranoside. Absorbance measurements on the fractions collected from the column enabled us to determine the amount of free pigment as a percentage of the total amount of chlorophyll in the stock solution.

Time-resolved fluorescence. Excited singlet-state lifetimes were measured using the technique of time-correlated single-photon counting [18]. The apparatus consisted of a mode-locked Coherent CR-6 argon-ion laser synchronously pumping a cavity-dumped rhodamine 6-G dye laser. The system provided variable repetition rate (single-shot to 92 MHz), tunable (590–630 nm) pulses of width approx. 10 ps (as measured by autocorrelation). A more detailed description of the apparatus may be found in Refs 19 and 20.

The recorded decay profile, $F(t)$, may be described in terms of a convolution of the molecular response to delta-function excitation, $i(t)$, and the instrument response function, $g(t)$, as shown in Eqn. 1:

$$F(t) = \int_{t'=0}^{t'=t+\delta} i(t+\delta-t')\,g(t')\,\mathrm{d}t' + C \qquad (1)$$

where δ is the shift in the zero time between the excitation function and the decay curve. This shift may result from pump-pulse instability or, as is most often the case, from the variation of the average transit-time spread of electrons in the photomultiplier tube. C is a constant which corresponds to the background noise level arising from spurious random electron pulses in the photomultiplier. Both δ and C are left as variable parameters in the least-squares analysis of the data to allow fitting over all the data.

Assuming a biphasic fluorescence decay, the function $i(t)$ takes the form of Eqn. 2:

$$i(t) = a_1\,\mathrm{e}^{-t/\tau_1} + a_2\,\mathrm{e}^{-t/\tau_2} \qquad (2)$$

where a_1 and a_2 are pre-exponential weighting factors and τ_1 and τ_2 are 1/e-decay times.

The absolute values of the pre-exponential factors depend upon the precise experimental conditions employed. Relative amplitudes, however, are of more use in that they can yield information about the relative numbers of molecules associated with each decay lifetime. In this work only

relative amplitudes are used to derive any information about the systems under study.

The instrument response function of the apparatus was determined to be approx. 460 (±10) ps. From this figure it was estimated that the equipment was capable of resolving decays as short as 150–200 ps. In order to avoid effects due to pulse-pile up [21], the count rate was never higher than 10 kHz (approx. 1 photon detected every 500 pulses). The pulses were attenuated using neutral density filters so that the average pulse intensity was approx. 10^9 photons per pulse per cm^2. Under these conditions it was assumed that effects due to singlet–singlet annihilation were negligible [22]. Effects due to the anisotropy of the observed fluorescence were removed by inserting a linear polariser in front of the monochromator slit at 54° 22′ with respect to the polarisation of the excitation beam. When necessary scattered excitation light was removed from the fluorescence by the use of suitable interference filters (Balzers, 40 nm).

In order to test that the equipment was functioning under conditions approximating those used for the samples under investigation, a monoexponential standard was chosen which had a similar lifetime and absorption/fluorescence spectral features as the LHC. The latter criterion is very important in order to ensure that the wavelength dependence of the instrument response function is not leading to reconvolution of the chosen model function with an incorrect response function [23]. This artefact is characterised by the inability of a convolved monoexponential model function to fit satisfactorily the rising edge of the experimentally obtained data, i.e., a single exponential fit to the fluorescence data from the standard is unacceptable as judged by the reduced χ^2 and other statistical criteria. By keeping the excitation and emission wavelengths as close a possible such distortions are minimised and, providing a good fit can be obtained with the standard under nearly actual sample conditions, it can be assumed that this particular artefact will not lead to an overfitting of the sample data. Clearly the choice of monoexponential standard is of critical importance in determining the reliability of the photophysical parameters extracted from the fluorescence decay of the sample.

10 μg/ml Chl *a* (obtained from Sigma Chemical Company) dissolved in diethylether plus 1% pyridine proved a satisfactory monoexponential standard for this work. The addition of pyridine ensured that the chlorophyll was ligated only to pyridine and not to water and that most of the chlorophyll was in a monomeric state [24]. The steady-state absorption, fluorescence and the lifetime of the standard did not differ markedly from Chl-*a* dissolved in ether in the absence of pyridine. A single exponential fit was always obtained for this sample with a decay time of 6.70 (±0.01) ns. The quantum yield of fluorescence for Chl-*a* in ether has been determined to be 0.32 [25] and the natural lifetime was estimated from the absorption spectrum to be 19.2 ns. The observed lifetime appears to correlate reasonably well with the value calculated by multiplying these parameters.

Data analysis of time-resolved fluorescence. Deconvolution was performed using least squares iterative reconvolution [26]. A search based on the Marquardt algorithm [27] was carried out to find the parameter increments which minimised the reduced χ^2.

Reduced χ^2 values close to unity and insignifi-

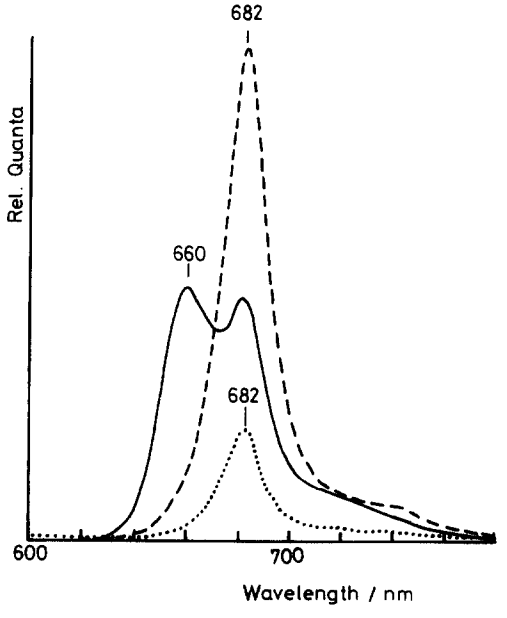

Fig. 1. Steady-state fluorescence emission spectra of the LHC in *n*-octyl-β-D-glucopyranoside several hours after preparation under high (———), medium (- - - - - -) and low (· · · · · ·) molar ratio conditions. Excitation wavelength: 470 nm.

cant correlation in the weighted residuals of a fit were deemed as reasonable criteria for the acceptance of a particular model function. All the decays had 20000 counts in the maximum channel, which, according to James and Ware [28], is sufficient to resolve complex underlying distributions of exponentials. However, a compromise had to be reached between better signal-to-noise ratios and distortions resulting from instrumental instability which become more important the longer counts are accumulated. Also, under conditions of higher total counts, it seems probable that the difference in the response functions at the excitation and emission wavelengths will be more marked as a result of the higher signal-to-noise levels. As discussed previously this can lead to serious errors in the data fitting particularly over the rising edge of the decay.

All the analyses were performed on a Jarogate Sprite microcomputer directly interfaced to an NS900 (Northern) multichannel analyser.

Results

Steady-state fluorescence

Fig. 1 shows the steady-state fluorescence emission spectra of the LHC under the three conditions shown in Table I recorded several hours after solubilisation from stock. Under high detergent/chlorophyll molar-ratio conditions (714 : 1 for triton X-100 and 5000 : 1 for *n*-octyl-β-D-glucopyranoside) we observed two peaks in the spectrum corresponding to Chl-*b* emission (660 nm) and Chl-*a* emission (682 nm). In contrast, the medium molar ratio case (44 : 1 for triton X-100 and 2173 : 1 for *n*-octyl-β-D-glucopyranoside) which corresponds approximately to the critical micelle concentration of both detergents showed a large single peak centred at 682 nm while a microcrystalline suspension of LHC and the low detergent/chlorophyll molar ratio case (4 : 1 for triton X-100 and 40 : 1 for *n*-octyl-β-D-glucopyranoside) gave rise to extensive fluorescence quenching as shown by the much reduced intensity of the emission at 682 nm. It was found that the three regimes corresponded to different molar ratios for the two detergents, triton X-100 and *n*-octyl-β-D-glucopyranoside. Qualitatively identical results were obtained in our spectroscopic studies on the LHC for the two detergents in their respective molar ratio regimes.

Fig. 2 shows the variation in the steady-state

TABLE I

DETERGENT CHLOROPHYLL MOLAR-RATIO CONDITIONS USED IN THIS STUDY

The relationship between these values and the critical micelle concentrations of the detergents is shown in parenthesis. OG, *n*-octyl-β-D-glucopyranoside; + and −, above and below critical micelle concentration (CMC), respectively.

Detergent/ chlorophyll ratio	Triton X-100 [a]	OG [b]
High	714 : 1 [c] ($+7.5 \cdot 10^{-3}$ M)	5000 : 1 ($+31 \cdot 10^{-3}$ M)
Medium	44 : 1 ($+0.24 \cdot 10^{-3}$ M)	2173 : 1 (at CMC)
Low	4 : 1 ($-0.194 \cdot 10^{-3}$ M)	40 : 1 $-23.5 \cdot 10^{-3}$ M)

[a] CMC = $3 \cdot 10^{-4}$ M [41].
[b] CMC = $2.5 \cdot 10^{-2}$ M [42].
[c] Detergent/chlorophyll molar ratio.

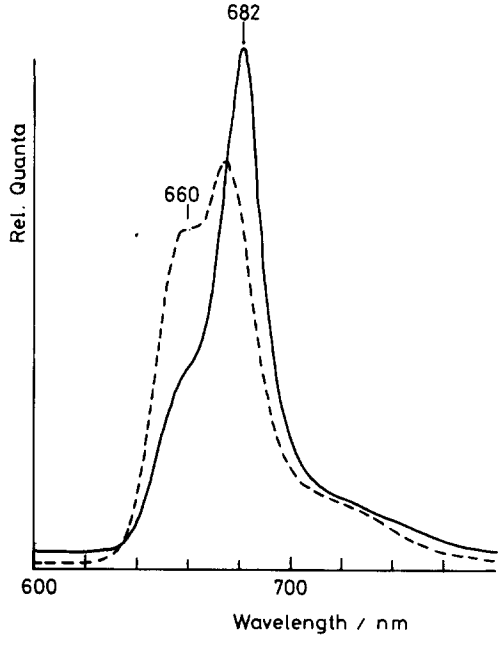

Fig. 2. Variation of the steady-state fluorescence emission spectrum of the LHC with time after preparation under high molar-ratio conditions in *n*-octyl-β-D-glucopyranoside. Immediately after preparation (———) and approx. 40 min after preparation (- - - - -). Excitation wavelength: 470 nm.

fluorescence emission of the LHC at different times after preparation under high detergent/chlorophyll conditions in *n*-octyl-β-D-glucopyranoside (see Table I). At times shortly after the preparation from stock we observed a main peak at approx. 682 nm corresponding to Chl-*a* emission and a small shoulder at approx. 660 nm corresponding to Chl-*b* emission. At longer times we observed a reduction in the intensity of the Chl-*a* emission with a concomitant grow in of the Chl-*b* peak. When the sample was left for several hours under these conditions the Chl-*a* peak practically disappeared while the Chl-*b* peak increased in amplitude (data not shown). In the medium detergent/chlorophyll condition the shape of the steady-state fluorescence remained unchanged for a period of days. Under low molar-ratio conditions the shape of the fluorescence emission also remained constant while the integrated area under the peak diminished slowly, i.e., the fluorescence yield dropped (data not shown).

Fig. 3 shows the invariance of the shape of the steady-state fluorescence emission of the LHC in *n*-octyl-β-D-glucopyranoside (under medium molar-ratio conditions) to different excitation wavelengths. At both the excitation wavelengths used we observed a single peak centred at 682 nm and there is no change in the shape of the peak. This invariance was also observed under low molar-ratio conditions whereas the high molar-ratio spectrum showed a marked shape dependence on the excitation wavelength used (data not shown).

Furthermore, it was observed that under high detergent conditions in triton X-100 the LHC showed a greater rate of 'grow in' of the 660 nm Chl-*b* feature than LHC solubilised in *n*-octyl-β-D-glucopyranoside. This was determined by monitoring the steady-state fluorescence emission in both detergents at periodic intervals (data not shown). Thus, the LHC is less stable when solubilised in triton X-100 than in *n*-octyl-β-D-glucopyranoside.

Time-resolved fluorescence: single-photon counting studies

Table II shows the results of fitting the fluorescence data in the three molar-ratio conditions for both detergents. In summary, the high molar-ratio condition in *n*-octyl-β-D-glucopyranoside yields complex fluorescence decay kinetics with a major component have a (1/e) lifetime of 5.50 (±0.16)

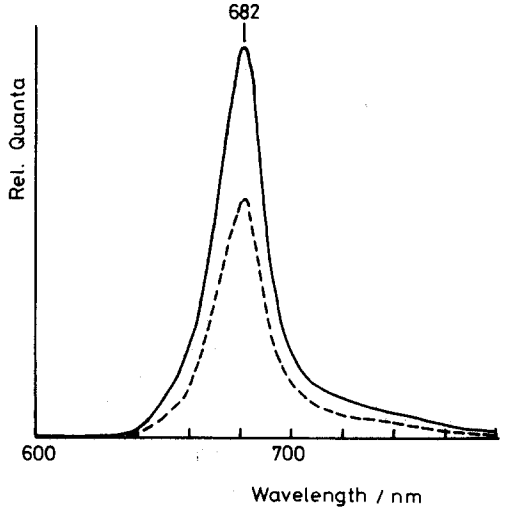

Fig. 3. Invariance of the shape of the steady-state fluorescence emission spectrum to excitation wavelength for the LHC in *n*-octyl-β-D-glucopyranoside under medium molar-ratio conditions. Excitation wavelengths: 470 nm (———) and 600 nm (- - - - - -).

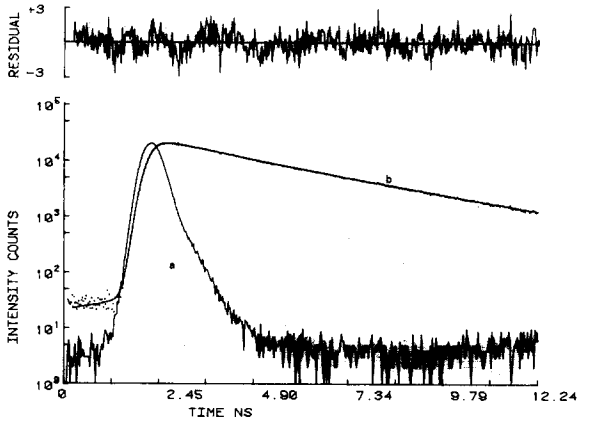

Fig. 4. Single photon-counting data obtained from the LHC prepared under medium molar-ratio conditions in *n*-octyl-β-D-glucopyranoside. Reduced $\chi^2 = 1.19$; biexponential fit with 1/e-lifetimes of 3.6 and 1.2 ns and pre-exponential factors in a ratio of approx. 4:1, respectively; excitation and emission wavelengths: 605 and 675 nm, respectively. (a) Excitation pulse profile (instrument response to near δ-function excitation). (b) Fluorescence response and a non-linear least-squares fit to the data.

TABLE II

SINGLE-PHOTON COUNTING FLUORESCENCE DECAY DATA

These data are obtained for the LHC under the three molar-ratio conditions, in a crystalline suspension and for the monoexponential standard, chlorophyll *a* in diethylether. OG, *n*-octyl-β-D-glucopyranoside.

Sample	Detergent	Number of decays	Molar ratio	Pre-exponential factors: 1/e-decay times (ns)					
				a_1	a_2	a_3	t_1	t_2	t_3
Chl-*a*/*b* complex	OG	4	high	1.46 (±0.16) [a]	0.835 (±0.13)	0.45 (±0.19)	5.50 (±0.16)	3.38 (±0.32)	0.14 (0.05)
	OG	8	medium	1.36 (±0.11)	0.37 (±0.02)		3.53 (±0.04)	1.12 (±0.12)	
	OG	2	low	0.36 (±0.20)	0.58 (±0.30)		0.38 (±0.10)	0.14 (±0.40)	
Chl-*a*/*b* complex	triton X-100	1	high	2.29			5.8		
	triton X-100	2	medium	1.47 (±0.40)	0.97 (±0.14)		3.32 (±0.18)	1.0 (±0.36)	
	triton X-100	1	low	not resolvable; est. lifetime(s) < 200 ps					
Chl-*a*/*b* complex	triton X-100	4	Crystalline suspension	1.29	2.6		0.65	0.33	
Chl *a*/ ether/ pyridine (standard)		20		1.80 (±0.01)			6.80 (±0.01)		

[a] Value in parenthesis is the standard error.

ns and two smaller components with lifetimes of approx. 3.3 (±0.3) and 0.15 (±0.05) ns. The medium molar-ratio regime consistently gave rise to a biexponential decay with lifetimes of 3.53 (±0.04) ns and 1.12 (±0.12) ns and pre-exponential factors in a ratio of approx. 4:1. The low molar-ratio and the suspension of the microcrystalline LHC yielded sub-nanosecond fluorescence data of an uncertain form though reasonable fitting was achieved to a biexponential model function with lifetime values of approx. 0.65 and 0.33 ns for the crystalline suspension. The determination of accurate values of the lifetimes in the latter case was difficult because of the limiting time resolution of the equipment. Fig. 4 shows actual single-photon counting data obtained under the medium molar ratio condition in *n*-octyl-β-D-glucopyranoside.

In triton X-100 the high molar-ratio condition yields a monophasic decay with a lifetime of 5.8 ns. The medium detergent regime yielded a biphasic decay with lifetimes 3.32(±0.18) and 1.0(±0.36) ns with pre-exponential weighting factors in a ratio of approx. 1.5:1. The low detergent/chlorophyll ratio gave very short decay times (< 200 ps) of uncertain decay function complexity.

Circular-dichroism spectra

Both Q-band and Soret region CD spectra were recorded for the LHC under the three detergent/chlorophyll conditions. In addition, the CD spectra of suspended microcrystalline LHC and LHC prepared in 1% SDS were measured.

In the medium molar-ratio regime we observed the following stable excitonic features in the Soret absorption region (Fig. 5): (1) a Chl-*b* exciton feature: approx. CD extrema at 445 nm (+) and 495 nm (−); (2) a Chl-*a*/*b* exciton feature: approx. CD extrema at 433 nm (+) and 477 nm (−); (3) a smaller excitonic feature approximately centred on the Chl-*b* (B_y) absorption maximum: approx. CD extrema at 487 nm (+) and 461 nm (−). This feature strengthened in the low molar-

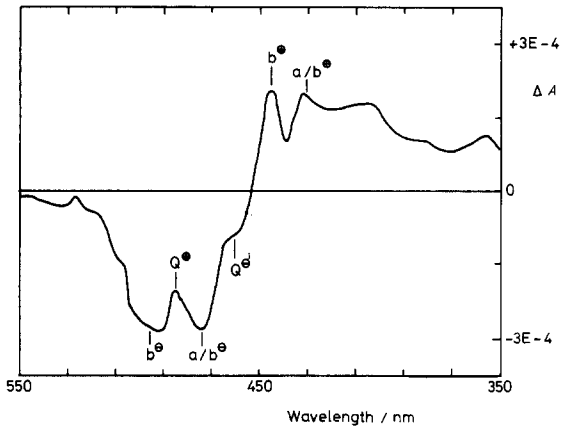

Fig. 5. Soret CD spectrum of the LHC in *n*-octyl-β-D-glucopyranoside under medium molar-ratio conditions, showing the main Chl-*b* excitonic feature (b), the lower amplitude 'quenching' Chl-*b* exciton (Q) and the Chl-*a*/*b* exciton (a/b).

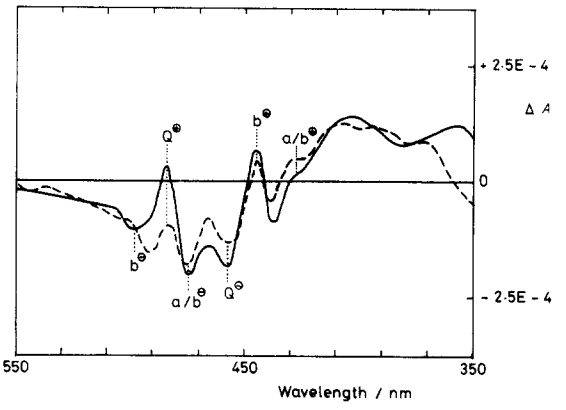

Fig. 7. Soret CD spectra of the LHC in a crystalline suspension (———) and under low molar-ratio conditions (- - - - - -) revealing qualitatively identical exciton features. The quenching exciton (Q) has gained in strength relative to the medium molar-ratio condition shown in Fig. 5, while the main Chl-*b* exciton (b) and the Chl-*a*/*b* exciton (a/b) have reduced amplitude.

ratio regime. The Q-band CD spectrum is characterised by a 'W' shape which is non-conservative (see Fig. 6).

In the low molar-ratio regime the Soret CD revealed all the excitonic features observed in the medium molar-ratio condition (see Fig. 7). In addition there was substantial increase in the amplitude of the exciton feature corresponding to feature (3) above, which made its assignment to Chl *b* clearer. The whole of the Soret spectrum also underwent a distinct left-handed (negative) shift. The Q-bands revealed the same features as in the medium molar-ratio case, except for the presence of an additional Chl-*b* feature with extrema at 679 nm (+) and 641 nm (−) (see Fig. 8). The CD of the microcrystalline suspension of LHC revealed qualitatively identical Soret CD features to those

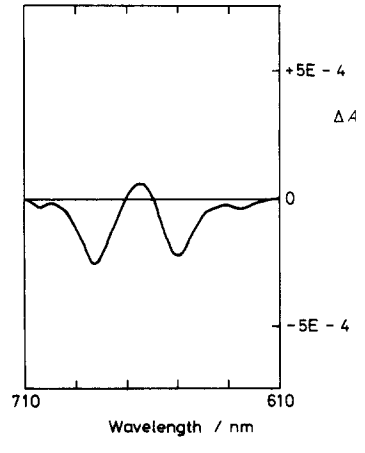

Fig. 6. Q-band CD spectrum of the LHC in *n*-octyl-β-D-glucopyranoside under medium molar-ratio conditions.

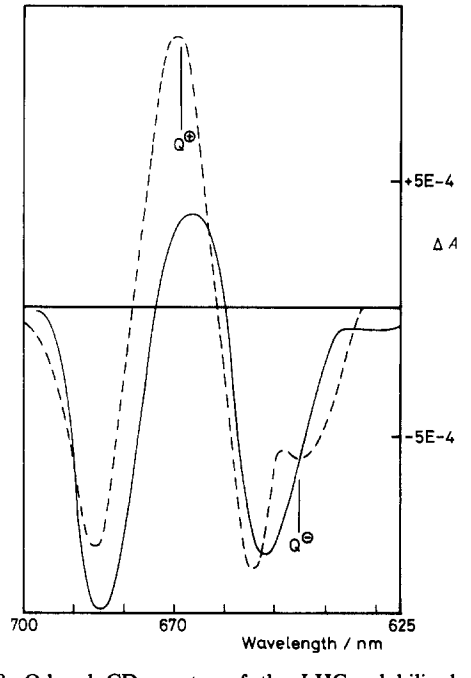

Fig. 8. Q-band CD spectra of the LHC solubilised under medium (———) and low (- - - - - -) molar-ratio conditions in *n*-octyl-β-D-glucopyranoside. The quenching associated exciton-feature (Q) is clearly evident.

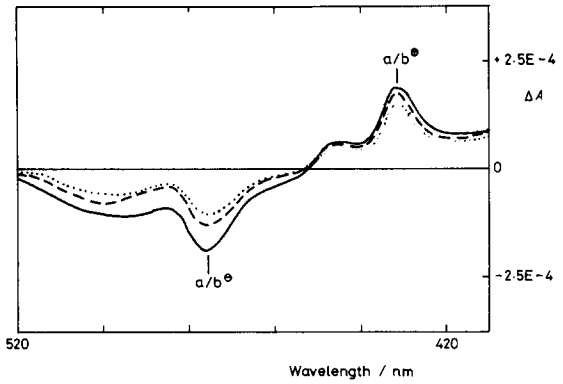

Fig. 9. Time variation of the Soret CD spectrum of the LHC under high molar-ratio conditions in *n*-octyl-β-D-glucopyranoside. The main Chl-*b* exciton feature is virtually absent, whilst the Chl-*a*/*b* exciton feature is prominent immediately after preparation (———) but slowly decreases in magnitude on standing (- - - - - -) 20 min (· · · · · ·) 40 min after preparation.

observed in the low molar-ratio condition (see Fig. 7).

In the high molar-ratio condition the Soret CD spectra showed that the Chl-*a*/*b* exciton (feature (2) above) was essentially unchanged at early times after preparation from stock (see Figs. 9 and 10). By contrast, the strength of the Chl-*b* feature (feature (1)) was considerably reduced. The whole spectrum gradually decayed with time as shown in Fig. 9. Eventually after a period of hours all that remained could be ascribed to intrinsic chlorophyll CD.

Fig. 10 also shows the Soret CD spectrum of the LHC prepared in 1% SDS. This spectrum shows a strong Chl-*b* feature (feature (1) above), while the Chl-*a*/*b* feature is virtually absent.

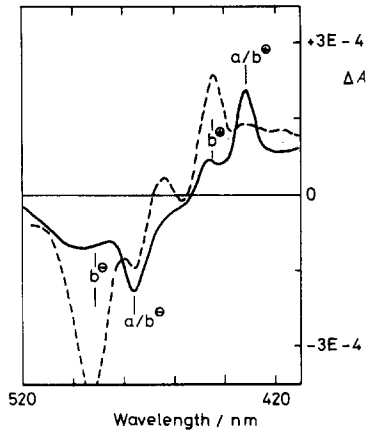

Fig. 10. Soret CD spectrum of the LHC solubilised in 1% SDS (- - - - - -) and under high molar-ratio conditions (———). The SDS dramatically reduces the strength of the Chl-*a*/*b* exciton feature (a/b) without affecting the purely Chl-*b* excitons (b). Under the high molar-ratio condition using *n*-octyl-β-D-glucopyranoside or triton X-100 the converse is true, the Chl-*a*/*b* feature remaining unaffected, whereas the Chl-*b* excitons are virtually removed.

Assignment of exciton features to circular dichroism spectra

The assignment of the excitonic interactions is based on the following observations.

(1) The centre of gravity for the exciton splitting is taken as the average transition energy. Thus the Chl-*b* features have their splitting centred on the Chl-*b* absorption maximum, while the Chl-*a*/*b* excitons have their splitting centre exactly mid-way between the Chl-*a* and Chl-*b* absorption maxima, see Fig. 11.

(2) All the exciton features are apparently additive with no noticeable interactive element. Thus removing one or other of the exciton features, by using the appropriate conditions, allows the position of the splitting centre to be determined with greater precision.

(3) The assignment of the major Chl-*b* feature to a C_3 symmetric Chl-*b* arrangement is based on other workers' interpretation of the data for SDS-solubilised LHC where these excitons are the only

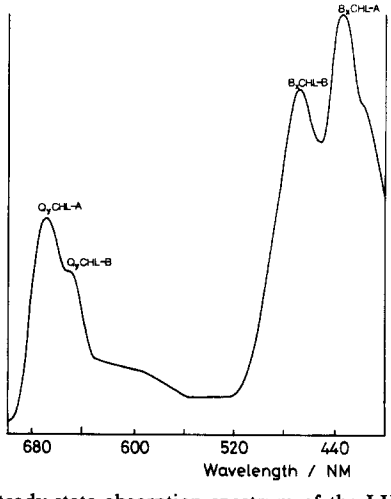

Fig. 11. Steady-state absorption spectrum of the LHC solubilised in *n*-octyl-β-D-glucopyranoside under medium molar-ratio conditions.

ones present [14,15,31]. The assignment to a C_3 arrangement is based on fluorescence depolarisation data. Our own fluorescence polarisation data (unpublished data) also shows extensive depolarisation of the fluorescence and we thus accept the assignment of the CD doublet to a C_3 symmetric chromophore arrangement.

Column chromatography

An estimate of free chlorophyll in solution at high and medium detergent/chlorophyll ratios was obtained by passing the solutions through a DEAE anion-exchange column (see Materials and Methods) approx. 1 h after the solutions were prepared from stock. At a detergent/chlorophyll ratio of 2173 : 1 in *n*-octyl-β-D-glucopyranoside, 7% of the chlorophyll passed through the column indicating that most of the chlorophyll-protein complex was intact. At a detergent/chlorophyll ratio of 5000 : 1 in *n*-octyl-β-D-glucopyranoside, however, only about 30% of the chlorophyll remained bound to the column, indicating that 70% of the chlorophyll had become detached from the complex under these conditions.

Discussion

Steady-state fluorescence

If Chl-*b* to Chl-*a* energy-transfer occurs efficiently under steady-state excitation conditions, i.e., not disrupted or slowed down to time-scales comparable with the fluorescence lifetime of Chl *b*, then we expect to see thermal equilibration of the absorbed excitation density on the chlorophyll molecules prior to fluorescence emission. At room temperature, the Boltzmann-weighted population of excited states gives a value of the order 10 : 1 for the excited-state concentration ratio of Chl *a*/Chl *b*. At equilibrium, therefore, we expect to observe a single peak in the fluorescence emission centred at the Chl-*a* emission maximum (682 nm) together with a small side band to the blue due to Chl-*b* emission (660 nm). In fact, the lower quantum yield of fluorescence of Chl *b* (0.12 in ether [25]) compared with that of Chl *a* (0.32 in ether [25]) renders this side band practically unobservable. Furthermore, in the absence of any disruption effects on the energy transfer, we expect to observe a fluorescence emission peak whose shape is invariant to the excitation wavelength. From the steady-state fluorescence emission spectra (Fig. 1) it is clear that the three molar-ratio regimes correspond to different states of the detergent solubilised pigment-protein complex.

Crystalline aggregated LHC and the in vivo state

Our interpretation of the results have been made in light of the known geometry of the crystallised LHC in 2-dimensional crystals [7]. Electron microscopy of the microcrystalline suspensions of LHC used in this work has shown that the aggregates present are stacks of 2-dimensional LHC crystals with a p321 plane group. In the low molar-ratio condition we observe quenching of the fluorescence yield (Fig. 1) and lifetime(s) of the LHC (Table II). In view of the similarity between the CD spectrum of the microcrystalline suspension and that of the low molar-ratio condition LHC (Fig. 7), we relate our observations in the latter case to the formation of microcrystalline aggregates of C_3 symmetric Chl-protein complexes. The exact values of the fluorescence lifetimes in both cases differ though they are all subnanosecond. The formation of aggregates of the LHC under these conditions occurs because the detergent concentration is below the critical level for micelle formation. When the detergent concentration is at or above the critical micelle concentration then the most important factor determining the state of the LHC is the ratio of detergent to chlorophyll. Assuming that the low detergent LHC aggregate has a similar structure to that of the 2-dimensional microcrystalline aggregates, we conclude that neither case correspond to the in vivo state of the LHC because Andersson et al. [29] have determined that the native thylakoid membrane is asymmetric with respect to the direction of insertion of the LHC complexes. Furthermore, it is highly unlikely that an in vivo state of the LHC would have such a low quantum yield of fluorescence (by comparison with the medium-detergent solubilised state) because this would considerably reduce the photochemical trapping efficiency in the membrane. A notable feature of the CD spectrum in the low molar-ratio condition (Fig. 7) when compared with the medium molar-ratio case (Fig. 5) is the apparent increase in amplitude of the extra Chl-*b* excitonic feature

(feature (3)). We attribute this CD signal to a new coupling of the Chl-*b* molecules induced by aggregation. We refer to this feature as the Chl-*b* 'quenching' exciton because it is possible that this new interaction is responsible for the quenching of the fluorescence by acting as a trap for excitons in a manner similar to that of some chlorophyll aggregates [30]. Even if these exciton states are not directly responsible for fluorescence quenching, their appearance always indicates aggregation of the LHC and the enhancement of the quenching mechanism.

Interpretation of the Soret circular dichroism

All the features of the CD spectra in the Soret region are approximately conservative and doublet in structure, i.e., correspond to transitions to exciton states of two different energies. This spectral signature can be explained in terms of either a dimeric or a C_3 symmetric chromophore interaction. The simplest C_3 symmetric interaction results from a 3-fold chromophore arrangement though a larger number of chromophores in a C_3 or C_6 arrangement could result in a similar CD spectrum (Drake, A., personal communication).

In general the dipole transition moments corresponding to the exciton states of a trimer without a C_3 axis are not orthogonal to each other. A C_3 symmetric chromophore trimer geometry, however, imposes orthogonality on the dipole moments and also ensures that a doublet will appear in the CD spectrum, i.e., two of the exciton states are degenerate. In general, for a non-C_3 symmetric trimer geometry we would expect three non-degenerate exciton states and hence a triplet in the CD spectrum [14]. In all the CD spectra (except at late times in the high molar-ratio condition, Fig. 9) we observe a large signal doublet Chl-*b* excitonic feature (feature (1) – see Results). This has been observed by other workers and is currently interpreted from fluorescence depolarisation data as being due to the presence of a C_3 symmetric Chl-*b* trimer chromophore interaction [14,15]. In view of the fact that the LHC forms aggregates of C_3 symmetric protein trimers [7], it seems reasonable to associate the C_3 chromophore geometry of the chlorophyll-*b* exciton feature with the C_3 axis of symmetry of the trimer. There are no other C_3 symmetric geometries visible at 16 Å resolution.

Assignment of decay times: medium detergent conditions

Under medium molar-ratio conditions the steady-state fluorescence suggests that energy transfer between Chl *b* and Chl *a* is both efficient and unaffected by the detergent environment over relatively long time scales. We believe that this stable state of the LHC corresponds most closely to the in vivo condition of the LHC complex in the thylakoid membrane. We propose that our biphasic fluorescence decay data from the LHC under these conditions can be explained in terms of heterogeneity with respect to the aggregation state of the solubilised LHC units in vitro. This conclusion is supported by the CD spectra of the LHC solubilised under medium molar-ratio and low molar-ratio and in microcrystalline conditions. The presence of the small signal Chl-*b* 'quenching' exciton (feature (3) – see Results) in the medium molar-ratio CD spectrum suggests the presence of a small amount of aggregate even under the medium detergent conditions. The biphasic fluorescence data has characteristic (1/e) decay times of 3.3–3.5 ns and 1–1.1 ns. Assuming an approximately constant radiative lifetime for Chl *a*, the ratio of the pre-exponential weighting factors (1.5–3.5 : 1) is an approximate measure of the relative number of Chl-*a* molecules in each state. Each state corresponds to a different average microenvironment of the molecules and is associated with a unique lifetime. The CD spectra and biochemical/crystallographic evidence suggests that the predominant state of the LHC under these conditions corresponds to solubilised non-aggregated chlorophyll-protein trimer complexes existing in separate micellar environments. If this is the case then the pre-exponential weighting factors suggest that we may assign the long (3–3.5 ns) lifetime component to the isolated trimer complexes. The shorter component can then be assigned to another state of the LHC consistent with a shorter lifetime and a 'quenching' Chl-*b* exciton feature in the CD spectra, i.e., some form of aggregated chlorophyll-protein complex. It is quite possible, however, that the 1 ns lifetime arises from another source such as the presence of a contaminating chlorophyll protein or alternatively a different LHC form.

Other circular dichroism observations

The CD spectra display some other interesting qualities. The non-conservative nature of the Q-band spectrum in the medium molar-ratio case may well be due to interband coupling with the Soret region which shows a compensatory positive feature to the blue of the chlorophyll-B bands. A similar scheme has been used by Gülen and Knox [31] in their C_3 symmetric interaction model. However, this effect over the Q-band and Soret regions appears to be connected with the Chl-*a*/*b* interaction, since the absence of the Chl-*a*/*b* exciton in the presence of 1% SDS (Fig. 10) makes the Q-band and Soret bands approximately conservative in their own right. The negative shift of the Soret CD bands in the low molar-ratio and the microcrystalline LHC suspension (with respect to the medium molar-ratio spectrum) can be attributed to a geometric factor imposed by the p321 symmetry of the crystalline unit cell. Also, features (1) and (2) (see Results) above do not noticeably interact, but are additive, since the removal of one leaves the other largely unaffected. It is clear therefore that they arise from the interactions of different sets of chromophores at different locations on the protein. Finally, in view of the different chromophore geometries responsible for these excitons it is surprising that they have the same rotational strength.

Other models

Our biphasic fluorescence decay data for LHC under medium molar-ratio conditions, agree well with other workers though interpretations differ. Lotshaw et al. [16] interpret their biphasic fluorescence decay in terms of two non-communicating pigment groups per functional unit. Their model assumes that the LHC units comprise: (a) one group of pigments made up of two Chl-*b* molecules interacting with a single Chl-*a* molecule; and (b) another group comprising two Chl-*a* molecules interacting with a single Chl-*b* molecule. If the Chl-*b* molecules in (a) are closely juxtaposed then the short component could be explained in terms of quenching of the molecular excitations due to their close proximity. Such an interaction would lead to a doublet CD signal at the Chl-*b* absorption maximum which is indeed observed. This model, however, does not agree with the fluorescence depolarisation data of Van Metter [14].

The Van Metter-Knox-Shepanski model of the LHC [14,15] is based upon a closely interacting exciton-coupled Chl-*b* trimer which transfer excitation energy to the Chl-*a* molecules. This model supposes that the Chl-*b* to Chl-*a* separation is sufficiently large or their relative orientation is such that significant excitonic interactions on absorption are negligible while maintaining efficient Förster energy-transfer. This would explain the absence of any CD signal at the midpoint of the Chl-*b*/Chl-*a* absorption maxima. The same is assumed to be true for Chl-*a*/Chl-*a* interactions. This model predicts monoexponential decay with a $1/e$ time equal to the excitation weighted average lifetime of the coupled system for localised excitons. Our CD results suggest however that some Chl-*b*/Chl-*a* interactions are significant for the LHC solubilised in triton X-100 and *n*-octyl-*β*-D-glucopyranoside resulting in excitonic coupling on absorption. For the purpose of comparison we also show the CD of the LHC in 1% SDS (see Fig. 10) from which it is evident that the effect of this anionic detergent is to remove the Chl-*b*/Chl-*a* excitonic interaction thus simplifying the overall CD spectrum. The process by which this happens is not clear, but it seems that Chl-*b*/Chl-*a* energy-transfer is still occurring (from steady-state fluorescence emission spectrum; data not shown) despite the apparent disruption of the chromophore interaction. From our results we cannot distinguish between the effect of detergent increasing the separation between chromophores or changing the relative orientation of the chromophore dipole transition moments as both could lead to a decrease in the excitonic interaction. A systematic study of the effect of different concentrations of SDS on the CD of the LHC has recently been reported by Gülen and coworkers [32] and our results are in good agreement with theirs.

Nordlund and Knox [22] have determined the lifetime of a purified aggregate form of the LHC and a solubilised non-aggregated form of the LHC. Using a signal averaging streak-camera system they obtained a monoexponential lifetime of 1.2 ($\pm$0.5) ns for the aggregated species and a monoexponential lifetime of 3.1 ($\pm$0.3) ns for the

solubilised form. Although the data quality is not as high as that achieved using single-photon counting we believe that these results add further support to the possible heterogeneity of solubilised LHC. We believe that the quantity of aggregated LHC present depends on the prevailing detergent/chlorophyll ratio, the age of the sample, the temperature and ion concentration. It is quite possible that under certain conditions little or no aggregate exists in the solution and thus we should expect a monoexponential decay time corresponding to the solubilised pigment-protein trimers.

A possible mechanism for LHC decomposition: high detergent / chlorophyll conditions

Fig. 9 clearly indicates that the LHC under high molar-ratio conditions is unstable and that major changes are occurring to the pigment protein complex on a time-scale of minutes. This is also supported by the excitation wavelength dependence of the structure of the emission and its variation over 40 min (data not shown). The column chromatography shows that under high molar-ratio conditions we observe a considerable amount of free chlorophyll which must have become detached from the protein. The CD spectra reveals some information about the mechanism of this process. It appears that the high detergent conditions disrupts the main Chl-*b* excitonic interaction (corresponding to a C_3 symmetric geometry of chromophores). From Fig. 9 it can be seen that this feature now carries reduced rotational strength. The Chl-*a*/*b* feature, however, is still prominent and remains so for approx. 1 h. On the assumption that the doublet Chl-*b* feature is a direct result of a C_3 symmetric chromophore interaction which itself derives from the C_3 symmetry of the protein, it seems reasonable to postulate that the initial effect of the detergent is to remove the C_3 symmetry of the protein to the extent that most of the trimers are broken up in to separate, unstable, monomer protein units. Clearly, it is still possible for these units to show strong Chl-*a*/*b* excitonic interaction, however, the latter has a time-dependence because of what we believe to be the instability of the protein monomers with respect to conformation and subsequent detachment of the protein ligated pigments. An alternative explanation, however, for the CD is that the detergent selectively disrupts the exciton coupling of the Chl-*b* trimer while leaving the protein geometry and the Chl-*b*/*a* exciton interactions relatively unaffected. We feel that this is a less likely explanation in view of the high detergent/chlorophyll ratio used which tends to result in predominantly dissociated chlorophyll-protein complexes as observed in SDS polyacrylamide gel electrophoresis [33].

The lifetime measurements under high molar-ratio conditions in *n*-octyl-β-D-glucopyranoside suggest that there is considerable chromophore heterogeneity with a major component (5.50 ± 0.16 ns) at 680 nm which corresponds to free Chl *a* in detergent micelle [34]. The middle component (3.38 ± 0.32 ns) could correspond to Chl *a* still ligated to a small amount of intact trimers (note that the main Chl-*b* feature has not disappeared completely) or it could correspond to Chl *a* attached to monomer protein prior to denaturation. The short component (0.146 ± 0.05 ns) could be artefact or some kind of aggregated Chl-*a* complex. In triton X-100, however, only a single lifetime (5.8 ns) was resolved under high detergent conditions. This difference in the number of components can be explained as follows. It was observed that the Chl-*b* emission increased at a greater rate in triton X-100 than *n*-octyl-β-D-glucopyranoside under high molar-ratio conditions. This suggests that protein denaturation and the release of free chlorophyll is faster in triton X-100 than *n*-octyl-β-D-glucopyranoside. All the lifetimes for the LHC were determined at approx. 10–15 min after solubilisation which was sufficient time for considerable denaturation of the LHC in triton X-100 but only sufficient to allow partial denaturation in *n*-octyl-β-D-glucopyranoside. As a result, only one long component was successfully resolved in triton X-100 (free Chl-*a*/micelle) whereas a multicomponent decay (assigned above) was recorded in *n*-octyl-β-D-glucopyranoside.

Il'ina et al. [13] have used phase fluorimetry and absorption measurements to investigate the interactions of both triton X-100 and SDS detergents with the LHC. They have measured a single 1/e-decay time (Υ) together with the relative quantum yield (Φ) and have used the ratio of the

two parameters (Υ/Φ) as a criterion for emission heterogeneity. Their findings are essentially in agreement with ours in as much as they find a variety of states of the LHC depending upon the exact detergent/chlorophyll conditions. They observe: quenching of the fluorescence lifetime and yield under conditions leading to aggregation; longer lifetimes in the moderate detergent regime, together with a changing (Υ/Φ) ratio as the detergent concentration increases, which suggests increasing emission heterogeneity; under high detergent concentrations free pigment is observed with a maximum lifetime of 5.8 ns and constant Υ/Φ ratio. They also observe marked changes in the lifetime over relatively small changes in total detergent concentration, e.g., an approximate two-fold increase in the lifetime (Υ) was obtained by increasing the detergent concentration by 0.01%. This correlates well with our general observation that a given state of the LHC is confined to a narrow range of detergent/chlorophyll ratios.

Relationship of LHC to CP II

Previous workers have used SDS polyacrylamide gel electrophoresis to extract the LHC from chloroplasts as first described by Thornber et al. [35]. The complex so obtained was designated as CP II and has been reported to contain 3 Chl-*a*, 3 Chl-*b* and one carotenoid molecule attached to a 35 kDa protein. All previous spectral information on the LHC has therefore been attributed to this complex. The recent work of Kühlbrandt [7] on the geometry of the crystalline LHC in 2-dimensional crystals and the spectral studies presented in this work suggest that this is not the case. CP II as described above, appears to exist for approx. 1 h under high detergent/chlorophyll conditions and is by no means the predominant state of the LHC in most of our experiments. We believe that the CP II corresponds to an unstable monomeric protein complex which does not exhibit the Chl-*b* excitonic feature in the CD corresponding to the C_3 Chl-*b* trimer, but does show a Chl-*a*/*b* excitonic feature in the CD for at least 1 h. In order to reconcile these observations with the CD data of other workers [14,15] we suggest that on resolubilisation of the LHC from the gel, re-formation of the monomer chlorophyll-protein complexes occurs such that the proposed in vivo C_3 symmetry of the LHC is restored thus giving rise to the observed CD spectrum. We do not, however, rule out the possibility that a stable form of the monomer could exist under certain conditions.

The in vivo state of the LHC

From our results we have been able to deduce the state of the LHC in vitro under different detergent conditions. We cannot, however, deduce anything directly about the state of the LHC in vivo because there is the possibility that the process of extraction from the thylakoid membranes, through solubilisation of the membrane protein, may have modified the state of the LHC. However, we believe that our stable in vitro form of the LHC is the most likely of the states observed to represent the in vivo condition of the LHC. Our belief is based upon the following. (1) The minimum, stable in vitro form of the LHC, corresponding to a C_3 symmetric protein trimer, is functionally active, i.e., Chl-*b* to Chl-*a* energy transfer is very efficient. (2) The unit cell for 2-dimensional crystals of the LHC has been determined to consist of two C_3 symmetric chlorophyll-protein complexes which are separated and inverted with respect to each other [7]. (3) Freeze-fracture analysis of mutants containing LHC have shown that the LHC corresponds to an 80 Å particle in the membrane. This is approximately the right size for a trimeric complex [36]. (4) 'Green gels' (mild SDS treatment) show two major LHC bands of approx. 70 and 25 kDa corresponding to the trimer and monomer, respectively [37].

It is interesting to speculate as to the functional significance of the proposed LHC C_3 protein symmetry in vivo. If this geometry is a necessary prerequisite for the exciton-coupled C_3 Chl-*b* chromophore arrangement, then it could be that the spherical symmetry of the transition moments of the exciton states of the trimer ensures that light, irrespective of polarisation, is absorbed by the trimer, that is, it acts as an isotropic absorber thus maximising the plants' light-harvesting efficiency. In this context, it is interesting to note that other antenna systems where the structure is known at atomic resolution show C_3 symmetry. A bacteriochlorophyll protein whose functional role in vivo is to mediate energy-transfer in *Prosthecochloris aestuarii* has been shown by X-ray

crystallography to consist of C_3 symmetric protein units comprising three identical subunits each containing seven bacteriochlorophyll molecules [38]. Similarly, the biliprotein C-phycocyanin from the cyanobacterium *Mastigocladus laminosus* has been shown to form C_3 trimers [39]. These are the basic units of the phycocyanin rods in the phycobilisome whose functional role is to funnel energy from sunlight to Chl *a* in the thylakoid membranes. The purple membrane of *Halobacterium halobium* has also been studied by X-ray and electron diffraction revealing three distinct threefold axes of rotational symmetry about which the protein molecules are arranged [40]. Each protein binds a single bacteriorhodopsin molecule and the CD suggests a strong excitonic interaction between a threefold arrangement of the bacteriorhodopsin chromophores.

Conclusions

We believe that in vitro the minimum stable functional unit of the LHC corresponds to a C_3 symmetric pigment-protein trimer complex. This complex exists in a variety of states in vitro depending upon the prevailing detergent/chlorophyll conditions. Under low molar ratio conditions we observe aggregation of the trimers resulting in quenched fluorescence yield/lifetime(s) associated with the formation of further Chl-*b* excitons in the aggregate. This new Chl-*b* interaction can be identified by a large amplitude conservative excitonic feature centred on the Chl-*b* Soret absorption maximum (and in the Q-bands). Under medium detergent/chlorophyll conditions, we believe that the majority of the trimers exist in separate micellar environments and are characterised by a lifetime of 3.53($\pm$0.04) ns. Our belief that this is the predominant protein state derives from a sequence of logical inferences obtained by combining our work on the LHC with the crystal structure determination [7] and biochemical evidence such as from gel electrophoresis [37]. A summary of our reasoning is as follows.

The CD of the LHC under medium molar-ratio conditions shows two sets of Chl-*b* excitons which differ in sign and in rotational strength by a factor of about 4–5 : 1, which agrees roughly with the relative pre-exponential weighting factors under these conditions. The smaller amplitude feature was attributed to aggregated LHC, and is revealed by comparing the CD spectra of the low (or crystalline) and medium detergent solubilised LHC. The short component in the fluorescence data (1.36 $\pm$ 0.11 ns) can be assigned to this species though the exact degree and/or order of aggregation appears to be different to that obtained under microcrystalline or low molar-ratio conditions because of the disparity in the lifetimes attributed to this state. The large Chl-*b* excitonic feature, which remains roughly invariant to a change from low to medium detergent conditions, appears to be intrinsic to a largely non-aggregated LHC state. The question remains, however, as to the nature of this state. We believe that the existence of separate, trimeric chlorophyll-protein complexes in the crystalline state is strong evidence that the trimers are capable of existing independently under suitable solubilisation conditions. Furthermore, there is strong biochemical evidence for trimeric protein complexes [36,37]. More indirect evidence suggesting that the trimer geometry is likely arises from Van Metter's fluorescence polarisation data [14], which implies that a C_3 symmetric chromophore arrangement exists in SDS-solubilised LHC, thus accounting for the doublet Chl-*b* CD signal (feature 1, see Results). It seems unlikely that the protein geometry and the Chl-*b* C_3 excitonic interaction are unrelated. It appears, therefore, that there is considerable circumstantial evidence to implicate isolated trimer complexes as the predominant LHC state under medium detergent conditions.

The observation of a doublet CD feature centred on the Chl-*b* Soret absorption maximum is in agreement with Van Metter's results [14] and when taken with his fluorescence depolarisation data suggests a closely interacting trimeric Chl-*b* chromophore arrangement. However, we also show that this model is a simplification because of the nature of the detergent used (SDS). We have shown that at 1% concentration SDS removes the excitonic coupling between neighbouring Chl-*b* and Chl-*a* molecules. This is in agreement with the work done by Gülen et al. [32]. The use of milder, non-ionic detergents shows that Chl-*b*/*a* interactions lead to a conclusive excitonic feature in the Soret CD and an extra feature in the

Q-band as well, though in the latter case the feature is not so easy to interpret. We postulate that the C_3 symmetry of the protein is a necessary prerequisite for the existence of the C_3 symmetric Chl-*b* chromophore arrangement. Under high detergent/chlorophyll conditions the CD suggests that the C_3 chromophore symmetry is broken, suggesting that the protein trimer splits into unstable monomeric units which we associate with the CP II form of the LHC. The monomers appear to last approx. 1 h, during which most of the chromophores detach from the protein. Chl-*b*-to-Chl-*a* energy transfer ceases and the main component of the fluorescence decay arises from Chl *a* in detergent micelle (5.5) ns lifetime [34].

Acknowledgements

We would like to express our thanks to Dr. A. Drake at the Chemistry Department of University College, London for his expert assistance in obtaining and interpreting the CD spectra. We would also like to thank Professor J. Barber (Department of Pure and Applied Biology, Imperial College, London) for his help and encouragement of this work. J.P. Ide would like to thank the U.S. Army for financial support during this work. L.B. Giorgi was supported by BP and D.R. Klug would like to thank the SERC for financial support.

References

1 Barber, J. (1985) in Topics in Photosynthesis, Vol. 6 (Barber, J. and Baker, N.R., eds.), Ch. 3, pp. 91–134, Elsevier, Amsterdam
2 Förster, T. (1965) in Modern Quantum Chemistry, part III (Sinanoglu, O., ed.), pp. 93–137, Academic Press, New York
3 Allen, J.F., Bennet, J., Steinback, K.E. and Arntzen, C.J. (1981) Nature 291, 1–5
4 Kyle, D.J., Kuang, T.-Y., Watson, J.L. and Arntzen, C.J. (1984) Biochim. Biophys. Acta 765, 89–96
5 Kyle, D.J., Staehelin, L.A. and Arntzen, C.J. (1983) Arch. Biochem. Biophys. 222, 527–541
6 Barber, J. (1980) FEBS Lett. 118, 1–10
7 Kühlbrandt, W. (1984) Nature 307, 478–479
8 Thornber, J.P. (1975) Annu. Rev. Plant Physiol. 67, 127–158
9 Mullet, J.E. (1983) J. Biol. Chem. 258, 9941–9948
10 Lee, J. (1985) Proc. Natl. Acad. Sci. USA 82, 386–390
11 Coruzzi, G., Broglie, R., Cashmore, A.R. and Chua, H.N. (1983) J. Cell. Biol. 258, 1399–1402
12 Dunsmuir, P., Smith, S.M. and Bedbrook, J. (1983) J. Mol. Appl. Gen. 2, 285–300
13 Il'ina, M.D., Kotova, E.A. and Borisov, A.Yu. (1981) Biochim. Biophys. Acta. 636, 193–200
14 Van Metter, R.L. (1977) Biochim. Biophys. Acta 462, 642–658
15 Shepanski, J.F. and Knox, R.S. (1981) Isr. J. Chem. 21, 325–331
16 Lotshaw, W.T., Alberte, R.S. and Fleming G.R. (1982) Biochim. Biophys. Acta 682, 75–85
17 Kühlbrandt, W., Thaler, T. and Wehrli, E. (1983) J. Cell. Biol. 96, 1414–1424
18 Knight, A.E.W. and Selinger, B.K. (1973) Aust. J. Chem. 26, 1–27
19 Fleming, G.R., Waldeck, D. and Beddard, G.S. (1981) Il Nuovo Cimento 63B, 151–172
20 O'Connor, D.V. and Phillips, D. (1984) in Time-Correlated Single Photon Counting, Ch. 2, Academic Press, London
21 Harris, C.M. and Selinger, B.K. (1979) Aust. J. Chem. 32, 2111–2129
22 Nordlund, T.M. and Knox, W.H. (1981) J. Biophys. 36, 193–201
23 Lewis, C., Ware, W.R., Doemeny, L.J. and Nemzek, T.L. (1973) Rev. Sci. Instrum. 44, 107–114
24 Connolly, J.S., Janzen, A.F. and Samuel, E.B. (1982) Photochem. Photobiol. 36, 559–563
25 Weber, G. and Teale, J.W.F. (1957) Trans. Faraday Soc. 53, 646–655
26 Ware, W.R., Doemeny, L.J. and Nemzek, T.L. (1973) J. Phys. Chem. 77, 2038–2048
27 Marquardt, D.W. (1963) J. Soc. Ind. Appl. Math. 11, 431–441
28 James, D.R. and Ware, W.R. (1986) Chem. Phys. Lett. 126, 7–11
29 Andersson, B., Anderson, J.M. and Ryrie, I.J. (1982) Eur. J. Biochem. 123, 465–472
30 Beddard, G.S., Carlin, S.E. and Porter, G. (1976) Chem. Phys. Lett. 43, 27–32
31 Gülen, D. and Knox, R.S. (1984) Photobiochem. Photobiophys. 7, 247–286
32 Gülen, D., Knox, R.S. and Breton, J. (1986) Photosynth. Res. 9, 13–20
33 Genge, S., Pilger, D. and Hiller, R.G. (1974) Biochim. Biophys. Acta 347, 22–30
34 Ide, J.P., Klug, D.R., Kühlbrandt, W., Giorgi, L.B., Porter, G., Gore, B.L., Doust, T. and Barber, J. (1986) Biochem. Soc. Trans. 14, 34
35 Thornber, J.P., Gregory, R.P.F., Smith, C.A. and Bailey, J.L. (1967) Biochem. 6, 391–396
36 Simpson, D.J. (1978) Carlsberg Res. Commun. 44, 305–336
37 Anderson, J.M., Waldron, J.C. and Thorne, S.W. (1978) FEBS Lett. 92, 227–233
38 Fenna, R.E. and Matthews, B.W. (1975) Nature 258, 573–577
39 Schirmer, T., Bode, W., Huber, R., Sidler, W. and Zuber, H. (1985) J. Mol. Biol. 184, 257–277
40 Kriebel, A.N. and Albrecht, A.C. (1976) J. Chem. Phys. 65, 4575–4583
41 Helenius, A. and Simons, K. (1975) Biochim. Biophys. Acta 415, 29–79
42 Camm, E.L. and Green, B.R. (1981) Plant Physiol. 67, 1061–1063